Published in final edited form as:
Invest Ophthalmol Vis Sci. 2009 August ; 50(8): 3985–3995. doi:10.1167/iovs.08-3364.

Age-dependent disease expression determines remodeling of the retinal mosaic in carriers of *RPGR* exon ORF15 mutations

William A. Beltran[1], **Gregory M. Acland**[2], and **Gustavo D. Aguirre**[1]

[1] Section of Ophthalmology, School of Veterinary Medicine, University of Pennsylvania, Philadelphia, PA 19104, USA

[2] James A. Baker Institute for Animal Health, College of Veterinary Medicine, Cornell University, Ithaca, NY 14853, USA

Abstract

Purpose—To characterize the retinal histopathology in carriers of X-linked progressive retinal atrophy (*XLPRA1* & *XLPRA2*), two canine models of X-linked retinitis pigmentosa caused, respectively, by a stop and a frameshift mutation in *RPGR*ORF15.

Methods—Retinas of *XLPRA2* and *XLPRA1* carriers of different ages were processed for morphologic evaluation, TUNEL assay, and immunohistochemistry. Cell-specific markers were used to examine retinal remodeling events.

Results—A mosaic pattern composed of patches of diseased and normal retina was first detected in *XLPRA2* carriers at 4.9 weeks of age. A peak of photoreceptor cell death led to focal rod loss; however, in these patches an increased density of cones was found to persist over time. Patches of disease gradually disappeared such that by 39 weeks of age the overall retinal morphology, albeit thinner, had improved lamination. In older *XLPRA2* carriers (≥8.8 years), extended regions of severe degeneration occurred in the peripheral/mid-peripheral retina.

In *XLPRA1* carriers, opsin mislocalization and rare events of rod death were detected by TUNEL assay at 20 weeks of age, however patchy degeneration was only seen by 1.4 years, and was still apparent at 7.8 years.

Conclusion—The time of onset and the progression of the disease differed between the two models. In the early onset form (*XLPRA2*) the morphologic appearance of the retinal mosaic changed as a function of age, suggesting that structural plasticity persists in the early postnatal canine retina as mutant photoreceptors die. In the late onset form (*XLPRA1*), patches of disease persisted until later ages.

INTRODUCTION

X-linked retinitis pigmentosa (XLRP) comprises some of the most severe forms of RP, and accounts for about 10–20% of familial cases.[1, 2] Six loci (RP2, RP3, RP6, RP23, RP24, RP34) have been associated by linkage analysis with XLRP; of these RP2 and RP3 are the two most common (www.retnet.org). Retinitis pigmentosa GTPase regulator (*RPGR*), the disease gene of the RP3 locus, accounts for > 70 % of the cases of X-linked retinitis pigmentosa (XLRP),[3–6] and exon ORF15, a mutational hot spot in *RPGR*, was shown to be mutated in 22–60% of XLRP patients.[3, 7, 8]

Corresponding author: William A. Beltran, School of Veterinary Medicine, University of Pennsylvania, Philadelphia, PA, 19104, USA; E-mail: wbeltran@vet.upenn.edu.

Mutations in *RPGR* can cause a spectrum of retinal diseases that include cone-rod dystrophies,[9] macular degeneration,[10] and more commonly rod cone degenerations.[11] Males affected with *RPGR*-XLRP typically exhibit night blindness in their first decade of life followed by reduction of their visual field, and loss of central visual acuity. By the end of their fourth decade most patients are legally blind.[12] Female carriers, on the other hand, display a broad spectrum of disease severity. The age of onset and the extent of fundus pigmentary changes, visual field defects and ERG abnormalities vary considerably between and within families.[11, 13–15] A characteristic of female XLRP carriers is the patchy nature of the disease expression when assessed by funduscopic examination, Goldmann perimetry[11, 16], multifocal ERG[17], and histopathology [16, 18–20]. This mosaic of normal and diseased retinal foci is best explained by Lyon's hypothesis of random X-chromosome inactivation that occurs at an early stage of female embryogenesis.[21]

Histopathological reports of the retinal lesions in XLRP carriers are scarce. Indeed, they are limited to that of four individuals, three of them carrying mutations in *RPGR*.[16, 18–20] Since these studies were conducted on postmortem retinas of older (> 75 years of age) patients, the findings represent histological alterations observed at an advanced stage of disease. For obvious reasons, access to retinal tissues from younger patients is likely to be even more limited, and currently hampers our understanding of the course of disease in XLRP carriers. The use of animal models with naturally occurring forms of X-linked retinal degeneration represents a valuable tool to examine whether in carriers the mosaic pattern of degenerate and normal retinal foci remains unchanged throughout the course of disease, or whether remodeling of these patches takes place.

In the dog, two distinct forms of X-linked retinal degeneration, termed *XLPRA1* and *XLPRA2*, have been characterized, and are caused, respectively, by a stop and a frameshift mutation in *RPGR* exon ORF15.[22]. The frameshift mutation causes an early and severe loss of photoreceptors (*XLPRA2*) that begins a few weeks after birth, while the stop mutation disease (XLPRA1) has a later onset (~11 months of age), and more gradual progression.[22–24] In both diseases, multiple patches of degeneration have been reported in carriers.[22, 24] In the current study, we have expanded the analysis of the retinal mosaic in *XLPRA1* and *XLPRA2* heterozygotes, and find focal lesions of photoreceptor disease and degeneration similar to those observed throughout the retinas of homozygotes. In addition, we report that the retinal mosaic disease pattern changes as a function of age in *XLPRA2* carriers, while no such retinal plasticity occurs in carriers of the later onset *XLPRA1* disease.

MATERIALS and METHODS

Animals

Twelve dogs were used for this study. This included 10 crossbred female *XLPRA2* carrier dogs (age range: 3.9 weeks to 10.3 years), and 2 crossbred female *XLPRA1* carrier dogs (age: 20 and 24 weeks). All dogs were bred at the Retinal Disease Studies Facility (RDSF, University of Pennsylvania, New Bolton Center, Kennett Square, PA), and their genotype was determined either from the known status of their progenitors, or from genetic testing for the disease-causing mutation.[22] All animals were anesthetized by intravenous injection of sodium pentobarbital, enucleated, and then euthanatized. All procedures involving animals were done in compliance with the ARVO Statement for the Use of Animals in Ophthalmic and Vision Research. In addition to the 12 dogs that were specifically bred for this study, archival retinal sections from 7 older carriers of *XLPRA1* (age range: 1.4 years – 7.8 years) were included (Table1). No experiments with tissues from wild-type (i.e. non-mutant) dogs were repeated in the current study as they had already been performed and reported in a previous publication.[23]

Retinal histology

The left eyes of 8 *XLPRA2* carrier dogs (age range: 3.9 weeks – 10.3 years) were used for morphologic examination of disease expression using plastic or OCT embedding (see Table 1: morphology). Tissues were processed for plastic embedding as previously reported, and using a similar protocol as for the archival tissues from the 7 *XLPRA1* carriers.[25] After enucleation, the globes, and then the posterior segments, were isolated and fixed following a sequential triple fixative protocol (3% glutaraldehyde-2% formaldehyde; 2% glutaraldehyde-1% osmium tetroxide; and 2% osmium tetroxide). The posterior segments were then trimmed into pieces that extended from the optic nerve head to the *ora serrata* along the superior and inferior meridians, dehydrated, and embedded in epoxy resin (PolyBed 812, Polysciences, Warrington, PA). Tissues were sectioned with glass knives at 1 μm with a 2065 Reichert Jung supercut microtome (Leica, Deerfield, IL), stained with azure II-methylene blue with or without a paraphenylenediamine (PPDA) counterstain.

Sections from both the superior and inferior meridians were examined with a 40X objective by light microscopy (Axioplan; Carl Zeiss Meditech, Oberkochen, Germany). The sections were examined in contiguous fields from the optic disc to the *ora serrata*. This included evaluation of the retinal pigment epithelium (RPE), the rod and cone outer (OS) and inner (IS) segments, the thickness and density of the outer nuclear and inner nuclear layers (ONL & INL). Quantitative measurements of the ONL were made in *XLPRA2* carriers in the central (site S1: 2,000 ± 500 μm from the optic nerve head), peripheral (site S3: 2,000 ± 500 μm from the *ora serrata*), and mid-peripheral (site S2: midpoint ± 500 μm between the optic nerve head and the *ora serrata*) regions. As most archival sections from the *XLPRA1* carriers did not contain either the optic nerve head or the *ora serrata*, the measurements were made at the extremities of the section and referred to as central and peripheral retina.

TUNEL assay

In 8 *XLPRA2* and 2 *XLPRA1* carrier dogs, one eye was processed to perform TUNEL assays and/or immunohistochemistry (Table 1: TUNEL, IHC). Following enucleation, a slit was made through the globe at the level of the *ora serrata*, and the entire globe was fixed in paraformaldehyde, cryoprotected, and embedded in optimal cutting temperature (OCT) medium as previously reported.[23]

Cryosections (7 μm thick) along the superior meridian were used for TUNEL assay following the manufacturer's protocol (*In situ* cell death detection kit, Roche, Indianapolis, IN), and stained with DAPI. Positive controls included sections pretreated with DNAse I (3 U/ml in 50 mM Tris-HCl, pH 7.5, 1 mg/ml BSA for 10 min at room temperature). For negative controls the terminal transferase enzyme was omitted from the TUNEL reaction mixture. Sections were examined from the optic disc to the *ora serrata* by epifluorescence microscopy with the 40X objective. TUNEL-labeled cells in the ONL were counted throughout the entire length of the section, i.e. from disc to *ora serrata*. In order to determine the proportion of photoreceptor cells that undergo cell death as a function of time, we expressed our results as the number of TUNEL-labeled photoreceptor cells per 10^6 μm^2 of ONL as previously reported.[23] The area of the ONL of each section was obtained by measuring the entire length of the ONL from optic disc to *ora serrata*, and multiplying it by the average thickness of the ONL throughout the section (mean value of the thickness measured in the 3 locations reported above). If focal thinning was present at the site, the closest adjacent site that was representative for the ONL thickness was measured. In areas of decreased photoreceptor density this method may slightly underestimate the proportion of cells that are TUNEL positive, but was selected because individual cell counts could not be determined on 7 μm thick DAPI stained cryosections. For each dog, this was done in triplicate with sequential sections from the superior meridian. The values were averaged and reported as mean ± SD.

Immunohistochemistry

Cryosections made along the superior retinal meridian of 8 *XLPRA2* and 2 *XLPRA1* carrier dogs were processed as described above and were used for fluorescent IHC. We used a battery of cell-specific antibodies, most of which already have been shown to specifically label the canine retina (see details in Table 2).[23] Since previous testing of RPGR and RPGRIP antibodies conducted in our laboratory failed to show any crossreactivity or specificity on dog retina, we did not include them in this study.[22] Cryosections (7–10 μm thick) were incubated overnight with the primary antibodies following a blocking step with 10% normal serum from the appropriate species. The antigen-antibody complexes were visualized with fluorochrome-labeled secondary antibodies (Alexa Fluor, 1:200; Molecular Probes, Eugene, OR). DAPI stain was used to detect cell nuclei. Slides were mounted with gelvatol, a medium composed of polyvinyl alcohol and DABCO (Sigma-Aldrich, St Louis, MO), and examined with an epifluorescent microscope (Axioplan). Images were digitally captured (Spot 4.0 camera), and imported into a graphics program (Photoshop; Adobe, Mountain View, CA) for display. Confocal microscopy was also used on a subset of sections to image discrete structural changes occurring in the outer segments. Confocal images were acquired on a Leica TCS-SP5 tunable confocal and MP system with a Leica DM 6000 CFS upright microscope (Leica Microsystems, Wetzlar, Germany) through a 40x oil lens (N.A. = 1.25). The specimens were excited at 488 nm supplied by an Argon laser. DAPI was excited with multi-photon at 720 nm produced by a Coherent Chameleon Ultra II Ti:sapphire pulse laser (Santa Clara, CA, USA).

RESULTS

Multifocal retinal degeneration

Retinal histopathology of *XLPRA2* carriers—At 3.9 weeks of age, no morphologic abnormalities could be seen in the maturing photoreceptors (Figure 1 A). The earliest alterations that could be detected by 4.9 weeks of age on 1 μm-thick plastic sections consisted in patchy areas of OS misalignment and disruption resulting in a weaker PPDA staining (Figure 1 B); occasional pyknotic nuclei also were seen. At 5.9 weeks, there was more prominent OS disorganization that resulted in a clearer demarcation between diseased and non-diseased foci (Figure 1 C). In diseased areas, rod cell density was decreased, yet consistently there was an increase in ONL thickness due to increase in inter-nuclear distance. By 26.1 weeks of age (Figure 1 D_1), there was a generalized thinning of the ONL. Patches of disease surrounded by structurally normal retina persisted, but they appeared to be fewer and of smaller size (Figure 1 $D_{2,3}$). This was even more obvious by 39 weeks of age. In older dogs (8.8 and 10.3 years) multifocal patches were rarely found, but end stage peripheral retinal atrophy that extended towards the mid-peripheral region was observed (Table 3). Differences were observed between the two aged dogs both in the location and the extent of the retinal damage. In the 8.8 year-old dog, severe peripheral retinal damage (total atrophy to 1–2 rows of nuclei in the ONL) was seen in the superior region extending up to 7,000 μm from the ora serrata. The central retina had a thin ONL (4 rows of nuclei), photoreceptors had enlarged and short IS, but maintained their OS. Inferiorly, severe retinal damage (0–2 rows of nuclei) was seen throughout the entire retinal section. No OS were visible inferiorly, and the RPE was either directly apposed to the external limiting membrane (ELM) or to shortened IS. In the 10.3 year-old dog the peripheral and mid-peripheral regions of the retina were also severely affected, yet photoreceptor loss was more prominent superiorly than inferiorly (Figure 1 $E_{1–3}$).

Retinal histopathology of *XLPRA1* carriers—Examination of H&E stained cryosections from a 20 and 24 week-old *XLPRA1* carrier did not reveal any morphologic alterations compatible with an ongoing disease process (Figure 2 $A_{1–3}$). The earliest age at which foci of disease were found was at the next time point, 1.4 years. These were observed throughout the retinal length and characterized by a local loss of OS, and a decrease in rod

density and ONL thickness (Figure 2 $B_{1–3}$). Beginning at 4.9 years of age and increasing with time, foci of increased cone density and rod loss were seen throughout the retina length (Figure 2 $C_{1–3}$). Similarly to that reported in affected animals,[24] substantial differences in disease severity were observed between carrier dogs of similar ages (e.g. dogs H6 and H74, see Table 4).

Immunohistochemical characterization of retinal disease in *XLPRA* carriers

Multifocal retinal disease in *XLPRA2* carriers—Cell specific markers for rods and cones were tested to determine whether they were differentially expressed in normal and diseased areas of the retina (Figure 3). Immunolabeling with rod opsin revealed alterations as early as 3.9 weeks of age that were similar to that previously reported in affected animals. [23] These consisted of rod opsin mislocalization to the IS and ONL, and rod neurite sprouting (Figure 3 A_1). However in the case of the carrier dogs examined in this study, these abnormalities had a multifocal distribution that overlapped with the areas of ONL thickening. DAPI labeling confirmed that areas of increased ONL thickness corresponded to areas of diseased rods (Figure 3 A_2). At 39 weeks of age the number of patches of rod opsin mislocalization and ONL thickening were considerably reduced (Fig 3 $B_{1–2}$). By confocal microscopy we also confirmed that in those regions where opsin was mislocalized, and the ONL thickened, rod OS were misaligned and disorganized (Fig 3 $C_{1–2}$).

Since cone opsins have been shown to mislocalize during the early phase of the disease in affected *XLPRA2* dogs we investigated whether this also occurred in carriers (Figure 4). Double immunolabeling with rod opsin and M/L opsin antibodies showed mislocalization of M/L cone opsin in young animals (3.9 – 12 weeks of age) in the same retinal patches where rod opsin was mislocalized (Figure 4 $A_{1–2}$). A peculiar finding that could be detected as early as 5.9 weeks of age was the increased density of M/L cones in the patches where rod opsin was mislocalized (Figure 4 $C_{1–3}$) A similar observation was made when labeling cones with human cone arrestin antibody (data not shown). In older animals (39 weeks), patches of M/L opsin mislocalization persisted despite a decrease in rod opsin mislocalization. Thus, there were fewer patches of rod opsin mislocalization than patches of M/L cone opsin mislocalization (data not shown), suggesting a possible loss of mutant rods and the persistence of diseased cones. The temporal pattern of S opsin labeling was slightly different since mislocalization, which also occurred in the areas where rod opsin mislocalized (Figure 4 $B_{1–2}$), was rarely seen after 12 weeks of age. No clumping of S cones was seen as with M/L cones. This was not surprising since there as fewer S cones than M/L cones in the canine retina.

At 26.1 weeks of age, phagocytic cells were frequently seen in the subretinal space of the degenerating patches, but not in the surrounding intact areas. Double immunolabeling with RPE65 and CD18 antibodies demonstrated that these cells were macrophages rather that detached RPE cells migrating into subretinal space. (Figure 5 A, B)

Because photoreceptor degeneration in affected *XLPRA2* dogs is associated with inner retinal remodeling, we investigated whether focal retinal disease altered the underlying inner retina in *XLPRA2* carriers. PKCα and Goα labeling showed a retraction of the dendrites of rod bipolar cells that synapse with the diseased rods. (Figure 6 A_1, asterisks). GABA IHC, which was used to label GABAergic amacrine cells as well as the inner plexiform layer (IPL), did not show any focal alterations in the areas of photoreceptor disease in either young or older animals (data not shown). Müller cell reactivity, which was evidenced by intense GFAP labeling, occurred in the patches of photoreceptor disease as early as 8 weeks of age, and was still intense at 12 weeks (Figure 6 $B_{1–2}$). At 26.1 weeks of age, radial extensions of GFAP labeling were considerably reduced, and by 39 weeks labeling was limited to astrocytes, and Müller cell end feet in the nerve fiber layer (data not shown).

Multifocal retinal disease in *XLPRA1* carriers

IHC experiments were limited to the two dogs (20 and 24 weeks old) that had their retinas embedded in OCT. A patchy pattern of rod opsin and M/L cone opsin mislocalization was seen at both ages (Figure 7). Although rod neurite sprouting was clearly visible, we did not observe a thickening of the ONL at the sites of disease as in the *XLPRA2* carriers. It is important to note that mislocalization of rod and M/L cone opsins occurred at an age when there are no structural abnormalities visible in the retina by light and electron microscopy in hemizygous males.[24] S opsin mislocalization was seen in both animals but was limited to the peripheral retina (data not shown). No abnormal pattern in PKCα or Goα labeling was observed either, and GFAP labeling was limited to astrocytes and Müller cell end feet (data not shown).

Kinetics of photoreceptor cell death

TUNEL assay was performed on *XLPRA2* carrier retinas to determine the course of photoreceptor cell death. Quantification of TUNEL-labeled photoreceptors in *XLPRA2* carriers showed a similar burst of cell death at 5.9 weeks of age (241–302 TUNEL-labeled cells per 10^6 μm^2 of ONL) as previously reported in affected *XLPRA2* dogs (Figure 8 A and [23]). Between 12 and 26.1 weeks of age, there was a significantly reduced and more constant rate of cell death. By 39 weeks of age only 2–8 TUNEL-labeled cells per 10^6 μm^2 of ONL were counted. To confirm that cell death was occurring within the foci of retinal disease, we examined sections that were TUNEL-labeled and processed for rod opsin IHC. Results showed that TUNEL-positive photoreceptors were only found in areas where rod opsin was mislocalized to the ONL (Figure 8B). In the 20 and 24 week-old *XLPRA1* carriers, a limited number of TUNEL-labeled rods were observed and were restricted to the foci of rod opsin mislocalization (Figure 8 C).

Remodeling of the retinal mosaic in *XLPRA2* carriers

Evident thinning of the ONL was seen in older carriers of *XLPRA2*, and, in addition, there also seemed to be fewer disease patches (Figure 9). To further substantiate the observation that the retinal mosaic appeared to remodel in the young adult dog, we determined the proportion of retinal length that was occupied by foci of retinal degeneration as a function of age. This was done, when possible, on sections from both the superior and inferior meridians. Our findings (Figure 9 $A_{1–2}$, B) show that at 5.9 weeks of age, large and numerous foci of disease occupy > 40% of the retinal sections, while their number and size decrease markedly with age. By 39 weeks of age, less than 10% of the retina appeared to contain patches of disease. With time, the irregular waviness of the vitreal aspect of the ONL disappeared (compare Figure 9 A_1 with Figure 9 A_2), but a substantial thinning was noted. At 39 weeks of age the ONL thickness (Superior: 36 ± 1 μm; Inferior: 38 ± 1 μm) was reduced to about 44–57% of that measured at 3.9 weeks of age (Superior: 82 ± 4 μm; Inferior: 67 ± 2 μm) (Figure 9 C). Further reduction in ONL thickness in a 10.3 year-old carrier suggests that rare events of photoreceptor cell loss persist beyond the 39 week time-point (Figure 9 C).

Immunohistochemistry confirmed these results by showing that in animals older than 26 weeks of age there was a significant decrease in the number and size of the patches of rod opsin mislocalization (compare Figure 3 B_1 with Figure 3 A_1). It also confirmed that the ONL was thinner but appeared more uniform in older animals (compare Figure 3 B_2 with Figure 3 A_2). In older animals, the cone mosaic remained irregular and focal areas of increased cone density frequently could be found (Figure 4 D_1). As early as 12 weeks of age, some of these high cone density patches were characterized by the clumping of the cell somas, which often resulted in multiple layers of cones in the ONL (Figure 4 $D_{2–3}$).

In the inner retina, the number of patches of dendritic retraction followed a similar time course as that of the patches of rod opsin mislocalization. By 39 weeks of age, these had become very

rare and the vast majority of the bipolar cells had a normal appearance (compare Figure 6 A_2 with Figure 6 A_1).

No such remodeling events of the retinal mosaic were seen in young *XLPRA1* carriers that express a later onset and more progressive form of disease.

DISCUSSION

A single report on the use of multifocal electroretinography in carriers of XLRP has shown that these patients experience a mosaic pattern of retinal dysfunction.[26] A similar multifocal pattern of disease has been confirmed by several histological observations of retinas from older heterozygotes.[16, 18–20] The current study examined the retinas in carriers of two canine models of *RPGR*-XLRP, and showed significant changes (summarized in Table 5) in the appearance of the retinal mosaic as a function of age, particularly in the early onset model. These remodeling events suggest that the young adult canine retina retains some degree of morphologic plasticity.

In carriers of *XLPRA2*, the time of disease onset was similar to that previously reported in affected animals (~4–5 weeks of age), and was also followed by a burst of rod cell death at 6–7 weeks of age. This further confirms our conclusion[23] that a model of constant or exponentially decreasing risk of cell death[27] does not apply to the kinetics of photoreceptor degeneration in *XLPRA2*.

Surprisingly, the peak value of TUNEL-positive cells in heterozygotes was very close to that found in affected animals (female homozygotes and male hemizygotes), both in timing and amplitude. In the context of random X-chromosome inactivation, we expected this value to be about 50 % of that found in affected dogs. This finding may, therefore, reflect the occurrence of primary skewed X-inactivation, a process that has been implicated in female carriers with X-linked mental retardation disorders and hemophilia A (For review see [28]). A noteworthy observation is that counts of TUNEL–positive cells in affected and carrier animals were similar but only at the time of occurrence of the peak of cell death. Indeed, at later time-points, values in carriers were ~ 50% of that reported in affected dogs. Thus, an alternative explanation could be that “mutant” photoreceptors undergoing degeneration may cause, through a bystander effect, the death of neighboring “normal” photoreceptors that are expressing the wild type allele. Such a non cell-autonomous mechanism of degeneration has been suggested to occur in the chimeric retina of a transgenic mouse line expressing both wild type and mutant (P347S) rhodopsin.[29] This may be caused through the release of a diffusible apoptosis-promoting factor.[30] If so, during the burst of photoreceptor death, there may be involvement of both intrinsic (mutation dependent) and extrinsic (toxic/apoptotic inducing factors) mechanisms of cell death.

When comparing the histopathological patterns between *XLPRA1* and *XLPRA2* carriers it is apparent that the mosaic gradually disappears in *XLPRA2* between 4.9 and 39 weeks of age, while it persists, until at least 7.8 years of age, in *XLPRA1*. This may be correlated with the time of onset of degeneration in these two diseases (*XLPRA2*: early onset; *XLPRA1* late onset), and the ability of the retina to undergo a “corrective” remodeling event. We hypothesize that this may be occurring in the *XLPRA2* carrier retina through tangential dispersion of photoreceptors expressing the wild type *RPGR* allele into the degenerating patches. Such an event may only occur during a short time-window that follows photoreceptor maturation in the dog, and may no longer be present in the “non-plastic” adult retina such as that of a 1.4 year-old *XLPRA1*. It is to be determined if post developmental tangential dispersion of photoreceptors also occurs in human carriers of XLRP as this may have practical implications for corrective gene therapy. Indeed, if rods and cones have the capacity to move to neighboring

regions of diseased retina, then there is a risk that a treated region may end up being depleted of its rescued photoreceptors to the benefit of surrounding non-treated areas. This could have applications for the treatment of carriers of XLRP by opting for pan-retinal, rather than localized delivery of the gene therapy construct.

The early onset and rapidly progressing disease that occurs in carriers and affected XLPRA2 dogs (homozygous females and hemizygous males) is thought to result from a toxic gain of function. The 2 nucleotide deletion (del1084–1085) in *RPGRORF15* causes a frameshift that modifies significantly the amino acid sequence by adding 34 basic residues, increases the isoelectric point, and prematurely terminates translation 71 amino acids downstream.[22] The 5 nucleotide deletion (del 1028–1032) in XLPRA1 introduces a premature stop codon that truncates the *RPGROR15* isoform from its 230 C-terminal amino-acids, and slightly decreases the isoelectric point.[22] The current hypothesis is that this leads to a loss of function of *RPGRORF15*, and that this isoform may not be critical for retinal development and maturation. A similar correlation between disease phenotype and individual mutations in *RPGR* has been reported in two mouse models of RPGR-XLRP.[31, 32]

Besides the difference in the severity and time course of the patchy degeneration, XLPRA1 carriers differed from XLPRA2 carriers by exhibiting variation in disease severity at similar ages. This has also been found in XLPRA1 affected hemizygous male dogs,[24] and is likely caused by the effect of modifier genes. No such modifiers have been yet identified, however, candidate genes *RPGRIP1*, *RANBP2*, *NPM1*, *PDE6D*, *NPHP5*, and *ABCA4* have been excluded.[33]

A question that was not addressed in the current study is whether the remodeling of the cytoarchitecture of the carrier retina is paralleled by some functional plasticity. By 39 weeks of age, despite a loss of ~ 50 % of rods, the lamination of the ONL and the morphology of rod bipolar cells appear to have recovered from the earlier phase of multifocal degeneration. This potentially suggests that rewiring of second order neurons to surviving (non-mutant) photoreceptors can occur. Assessing whether structural recovery leads to a period of improved retinal function is a worthwhile subject for future investigation.

Several immunohistochemical and morphologic alterations observed in both the *XLPRA1* and *XLPRA2* carrier dogs have also been reported in human patients.[34, 35] This includes the mislocalization of rod and cone opsins[16, 19, 20] which may underline the putative role of the *RPGR*ORF15 isoform in trafficking proteins from the IS to the OS. Double fluorescent IHC showed that mislocalization of rod and cone opsins occurred within the same patch of disease. This finding was unexpected since, during retinal development, rods and cones that are clonally derived from the same photoreceptor progenitor cell have a different pattern of dispersion. Rods get distributed along a radial column while cones are tangentially dispersed.[36, 37] The mislocalization of cone and rod opsins within a same patch could be explained by a defective developmental tangential dispersion of cones expressing the mutant *RPGR* allele. Alternatively, cone opsin mislocalization may be the consequence of a toxic bystander effect of the surrounding “mutant” rods on cones that express the wild type *RPGR* allele. The lack of an antibody raised against the mutant canine RPGR isoforms currently precludes us from further investigating this question.

Another common finding that was observed in *RPGR*ORF15 carrier dogs and in a human patient is the focal aggregation of cones.[19] This was easily recognized in older animals, and was often the only remaining histological criteria that could be used to define a patch of disease. Careful examination of the cone distribution showed an increased density of cones in the patches of disease as early as 5.9 weeks of age.

In *XLPRA2*, a "corrective" remodeling phase follows the initial burst of cell death, and leads to preserved retinal lamination despite a loss of approximately 50% of the rods by 39 weeks of age. However, this event is only transient and topographically restricted as large regions of degeneration/atrophy are found in the peripheral and mid-peripheral retina of older animals. A similar topographical distribution has been described in a human carrier.[19] Several mechanisms that are not mutually exclusive could explain this persistent loss of photoreceptors, and its regional predilection. It has recently been reported that in human fibroblasts at least 15% of all X-linked genes can escape random X chromosome inactivation.[38] This secondary skewing of X inactivation has been shown to be associated with aging, although it is likely to be species-, tissue- and locus- specific.[39, 40] Thus, it is possible that in older carriers of *XLPRA2*, reactivation of the silenced mutant *RPGR* allele may lead to a second wave of photoreceptor death. Another potential explanation is that there may be a minimal number of rows of photoreceptors necessary to sustain viability of these cells. If such is the case, then gradual thinning of the ONL throughout the retinal surface is bound to have a more severe impact on peripheral regions where the ONL is several rows of ONL thinner than centrally. Finally, this late phase of peripheral degeneration could potentially also be explained by the generation of new photoreceptors from progenitor cells located at the retinal margin. Several reports have suggested that this mechanism of photoreceptor renewal may not be limited to fish, amphibians and birds, but also may be found in mammals.[41] If this is the case in the canine retina, then newly formed photoreceptors expressing the mutant *RPGR* allele would not only undergo cell death but could also cause a detrimental bystander effect on "non-mutant" photoreceptors located in the peripheral retina.

A significant finding of this study is that the morphologic appearance of the retinal mosaic changes with time and, as a consequence, so do the histological criteria used to define patches of degeneration. This was clearly observed in *XLPRA2*, and may also occur in human carriers of early onset forms of XLRP. The clinical implication of the remodeling events that occur in the carrier retina is that, depending on the stage of the disease, it may be challenging to diagnose, both in animal models and human patients, the mosaic pattern via *in vivo* imaging techniques such as optimal coherence tomography. In the case of *XLPRA2*, OCT imaging in a 5.9 week-old carrier would potentially identify foci of increased and decreased ONL thickness corresponding respectively to patches of diseased and normal retina. On the other hand, examination at later stages would not show any mosaicism and would likely reveal either normal retinal lamination with generalized and uniform thinning of the ONL (e.g. 39 weeks of age), or prominent and extended retinal thinning with loss of lamination in the peripheral retina of much older animals (e.g. 10.3 years of age).

In summary, characterization of the morphological changes that occur in the carrier retina of two canine models of XLRP has established that prominent remodeling events occur throughout the course of the disease, and has demonstrated that the retinal mosaic shows a dynamic and evolving response pattern. It also supports the evidence that heterozygotes for *RPGR*-XLRP mutations may experience severe visual impairment.[19, 42] These results provide new insight to gene therapy approaches that can be used in both affected and carrier retinas.

Acknowledgments

The authors are grateful to Dr. Cheryl Craft (Univ. of Southern California, Los Angeles) for providing the human cone arrestin antibody, Dr. Lingli Zhang (School of Veterinary Medicine, Univ. of Pennsylvania, core Bio-imaging facility) for help with confocal microscopy, Julie Jordan for technical assistance, and Mary Leonard (Univ. of Pennsylvania Biomedical Art & Design facility) for the illustrations.

Supported by: NIH grants EY-06855, EY-13132, EY-17549 (The content is solely the responsibility of the authors and does not necessarily represent the official views of the National Eye Institute or the National Institutes of Health), the Foundation Fighting Blindness Individual Investigator Award and Center grants, the Fight for Sight Nowak family grant, Vision Research Center grant P30 EY-001583, Hope for Vision Foundation, the ONCE International Prize for

Biomedicine and R&D for New Technologies for the Blind, the Van Sloun Fund for Canine Genetic Research, and the University of Pennsylvania Research Foundation.

References

1. Bird AC. X-linked retinitis pigmentosa. Br J Ophthalmol 1975;59:177–199. [PubMed: 1138842]
2. Jay M. On the heredity of retinitis pigmentosa. Br J Ophthalmol 1982;66:405–416. [PubMed: 7093178]
3. Vervoort R, Lennon A, Bird AC, et al. Mutational hot spot within a new RPGR exon in X-linked retinitis pigmentosa. Nat Genet 2000;25:462–466. [PubMed: 10932196]
4. Bader I, Brandau O, Achatz H, et al. X-linked retinitis pigmentosa: RPGR mutations in most families with definite X linkage and clustering of mutations in a short sequence stretch of exon ORF15. Invest Ophthalmol Vis Sci 2003;44:1458–1463. [PubMed: 12657579]
5. Sharon D, Sandberg MA, Rabe VW, Stillberger M, Dryja TP, Berson EL. RP2 and RPGR mutations and clinical correlations in patients with X-linked retinitis pigmentosa. Am J Hum Genet 2003;73:1131–1146. [PubMed: 14564670]
6. Pelletier V, Jambou M, Delphin N, et al. Comprehensive survey of mutations in RP2 and RPGR in patients affected with distinct retinal dystrophies: genotype-phenotype correlations and impact on genetic counseling. Hum Mutat 2007;28:81–91. [PubMed: 16969763]
7. Breuer DK, Yashar BM, Filippova E, et al. A comprehensive mutation analysis of RP2 and RPGR in a North American cohort of families with X-linked retinitis pigmentosa. Am J Hum Genet 2002;70:1545–1554. [PubMed: 11992260]
8. Pusch CM, Broghammer M, Jurklies B, Besch D, Jacobi FK. Ten novel ORF15 mutations confirm mutational hot spot in the RPGR gene in European patients with X-linked retinitis pigmentosa. Hum Mutat 2002;20:405. [PubMed: 12402343]
9. Mears AJ, Hiriyanna S, Vervoort R, et al. Remapping of the RP15 locus for X-linked cone-rod degeneration to Xp11.4-p21.1, and identification of a de novo insertion in the RPGR exon ORF15. Am J Hum Genet 2000;67:1000–1003. [PubMed: 10970770]
10. Ayyagari R, Demirci FY, Liu J, et al. X-linked recessive atrophic macular degeneration from RPGR mutation. Genomics 2002;80:166–171. [PubMed: 12160730]
11. Lorenz B, Andrassi M, Kretschmann U. Phenotype in two families with RP3 associated with RPGR mutations. Ophthalmic Genet 2003;24:89–101. [PubMed: 12789573]
12. Sandberg MA, Rosner B, Weigel-DiFranco C, Dryja TP, Berson EL. Disease course of patients with X-linked retinitis pigmentosa due to RPGR gene mutations. Invest Ophthalmol Vis Sci 2007;48:1298–1304. [PubMed: 17325176]
13. Yokoyama A, Maruiwa F, Hayakawa M, et al. Three novel mutations of the RPGR gene exon ORF15 in three Japanese families with X-linked retinitis pigmentosa. Am J Med Genet 2001;104:232–238. [PubMed: 11754050]
14. Koenekoop RK, Loyer M, Hand CK, et al. Novel RPGR mutations with distinct retinitis pigmentosa phenotypes in French-Canadian families. Am J Ophthalmol 2003;136:678–687. [PubMed: 14516808]
15. Grover S, Fishman GA, Anderson RJ, Lindeman M. A longitudinal study of visual function in carriers of X-linked recessive retinitis pigmentosa. Ophthalmology 2000;107:386–396. [PubMed: 10690843]
16. Jacobson SG, Buraczynska M, Milam AH, et al. Disease expression in X-linked retinitis pigmentosa caused by a putative null mutation in the RPGR gene. Invest Ophthalmol Vis Sci 1997;38:1983–1997. [PubMed: 9331262]
17. Vajaranant TS, Seiple W, Szlyk JP, Fishman GA. Detection using the multifocal electroretinogram of mosaic retinal dysfunction in carriers of X-linked retinitis pigmentosa. Ophthalmology 2002;109:560–568. [PubMed: 11874762]
18. Szamier RB, Berson EL. Retinal histopathology of a carrier of X-chromosome-linked retinitis pigmentosa. Ophthalmology 1985;92:271–278. [PubMed: 3982806]
19. Aguirre GD, Yashar BM, John SK, et al. Retinal histopathology of an XLRP carrier with a mutation in the RPGR exon ORF15. Exp Eye Res 2002;75:431–443. [PubMed: 12387791]

20. Adamian M, Pawlyk BS, Hong DH, Berson EL. Rod and Cone Opsin Mislocalization in an Autopsy Eye From a Carrier of X-linked Retinitis Pigmentosa With a Gly436Asp Mutation in the RPGR Gene. Am J Ophthalmol 2006;142:515–518. [PubMed: 16935610]
21. Lyon MF. Gene action in the X-chromosome of the mouse (Mus musculus L). Nature 1961;190:372–373. [PubMed: 13764598]
22. Zhang Q, Acland GM, Wu WX, et al. Different RPGR exon ORF15 mutations in Canids provide insights into photoreceptor cell degeneration. Hum Mol Genet 2002;11:993–1003. [PubMed: 11978759]
23. Beltran WA, Hammond P, Acland GM, Aguirre GD. A frameshift mutation in *RPGR* exon ORF15 causes photoreceptor degeneration and inner retina remodeling in a model of X-linked retinitis pigmentosa. Invest Ophthalmol Vis Sci 2006;47:1669–1681. [PubMed: 16565408]
24. Zeiss CJ, Acland GM, Aguirre GD. Retinal pathology of canine X-linked progressive retinal atrophy, the locus homologue of RP3. Invest Ophthalmol Vis Sci 1999;40:3292–3304. [PubMed: 10586956]
25. Acland GM, Aguirre GD. Retinal degenerations in the dog: IV. Early retinal degeneration (erd) in Norwegian elkhounds. Exp Eye Res 1987;44:491–521. [PubMed: 3496233]
26. Fattal E, Bochot A. Ocular delivery of nucleic acids: antisense oligonucleotides, aptamers and siRNA. Adv Drug Deliv Rev 2006;58:1203–1223. [PubMed: 17097190]
27. Clarke G, Collins RA, Leavitt BR, et al. A one-hit model of cell death in inherited neuronal degenerations. Nature 2000;406:195–199. [PubMed: 10910361]
28. Clerc P, Avner P. Random X-chromosome inactivation: skewing lessons for mice and men. Curr Opin Genet Dev 2006;16:246–253. [PubMed: 16647851]
29. Huang PC, Gaitan AE, Hao Y, Petters RM, Wong F. Cellular interactions implicated in the mechanism of photoreceptor degeneration in transgenic mice expressing a mutant rhodopsin gene. Proc Natl Acad Sci U S A 1993;90:8484–8488. [PubMed: 8378322]
30. Seigel GM, Liu L. Inducible apoptosis-promoting activity in retinal cell-conditioned medium. Mol Vis 1997;3:14. [PubMed: 9479005]
31. Hong DH, Pawlyk BS, Shang J, Sandberg MA, Berson EL, Li T. A retinitis pigmentosa GTPase regulator (RPGR)-deficient mouse model for X-linked retinitis pigmentosa (RP3). Proc Natl Acad Sci U S A 2000;97:3649–3654. [PubMed: 10725384]
32. Hong DH, Pawlyk BS, Adamian M, Li T. Dominant, gain-of-function mutant produced by truncation of RPGR. Invest Ophthalmol Vis Sci 2004;45:36–41. [PubMed: 14691151]
33. Guyon R, Pearce-Kelling SE, Zeiss CJ, Acland GM, Aguirre GD. Analysis of six candidate genes as potential modifiers of disease expression in canine XLPRA1, a model for human X-linked retinitis pigmentosa 3. Mol Vis 2007;13:1094–1105. [PubMed: 17653054]
34. Li ZY, Kljavin IJ, Milam AH. Rod photoreceptor neurite sprouting in retinitis pigmentosa. J Neurosci 1995;15:5429–5438. [PubMed: 7643192]
35. Fariss RN, Li ZY, Milam AH. Abnormalities in rod photoreceptors, amacrine cells, and horizontal cells in human retinas with retinitis pigmentosa. Am J Ophthalmol 2000;129:215–223. [PubMed: 10682975]
36. Reese BE, Harvey AR, Tan SS. Radial and tangential dispersion patterns in the mouse retina are cell-class specific. Proc Natl Acad Sci U S A 1995;92:2494–2498. [PubMed: 7708672]
37. Reese BE, Necessary BD, Tam PP, Faulkner-Jones B, Tan SS. Clonal expansion and cell dispersion in the developing mouse retina. Eur J Neurosci 1999;11:2965–2978. [PubMed: 10457191]
38. Carrel L, Willard HF. X-inactivation profile reveals extensive variability in X-linked gene expression in females. Nature 2005;434:400–404. [PubMed: 15772666]
39. Wareham KA, Lyon MF, Glenister PH, Williams ED. Age related reactivation of an X-linked gene. Nature 1987;327:725–727. [PubMed: 3600770]
40. Migeon BR, Axelman J, Beggs AH. Effect of ageing on reactivation of the human X-linked HPRT locus. Nature 1988;335:93–96. [PubMed: 2457812]
41. Moshiri A, Reh TA. Persistent progenitors at the retinal margin of ptc+/− mice. J Neurosci 2004;24:229–237. [PubMed: 14715955]
42. Souied E, Segues B, Ghazi I, et al. Severe manifestations in carrier females in X linked retinitis pigmentosa. J Med Genet 1997;34:793–797. [PubMed: 9350809]

43. Zeiss CJ, Ray K, Acland GM, Aguirre GD. Mapping of X-linked progressive retinal atrophy (XLPRA), the canine homolog of retinitis pigmentosa 3 (RP3). Hum Mol Genet 2000;9:531–537. [PubMed: 10699176]

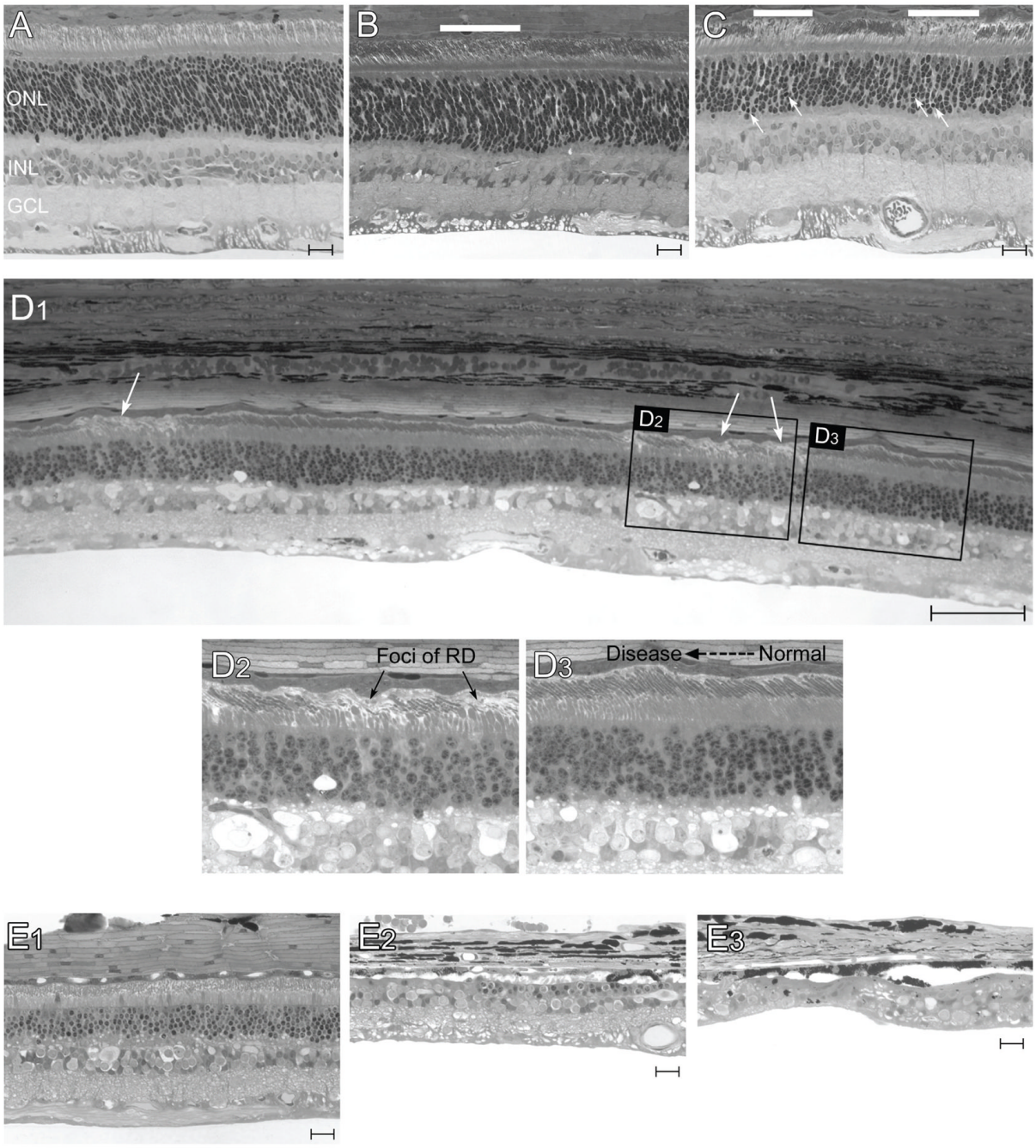

Figure 1.

Retinal morphology in carriers of *XLPRA2*. (**A**) Normal maturation of the retina at 3.9 weeks. (**B**) Early patch of outer segment misalignment (below white bar) and ONL thickening in a 4.9 week-old carrier. (**C**) Prominent foci of outer segment disruption in a 5.9 week-old carrier. Note the increased thickness of the ONL, decreased cell density and occasional pyknotic figures (arrows) in these patches. (**D_1**) Multifocal retinal degeneration in a 26.1 week-old carrier of *XLPRA2*. Foci of retinal degeneration (arrows) are surrounded by areas of normal retinal morphology. (**D_2**) High magnification of a patch of retinal degeneration. Note the misalignment and loss of photoreceptor outer segments, the shortening and broadening of the inner segments, and the decrease in cell density in the ONL. (**D_3**) High magnification at the transition zone of

a patch of retinal disease. Note the progressive disorganization of the inner and outer segments, and the decrease in chromatin compaction of the rods as one moves from a normal to a diseased area. (**$E_{1–3}$**) Retinal disease in a 10.3 year-old carrier of *XLPRA2*. (**E_1**) Despite a reduction in ONL thickness (approx 5–6 nuclei thick) in the central region, the retinal morphology appears well preserved in comparison to the severe retinal degeneration and complete retinal atrophy observed, respectively, in the mid-peripheral (**E_2**) and peripheral (**E_3**) regions. (Epoxy resin, 1 μm sections) Scale bars: (A–C, $E_{1–3}$) 20 μm; (D_1) 80 μm. Abbreviations: ONL = outer nuclear layer; INL = inner nuclear layer; GCL = ganglion cell layer.

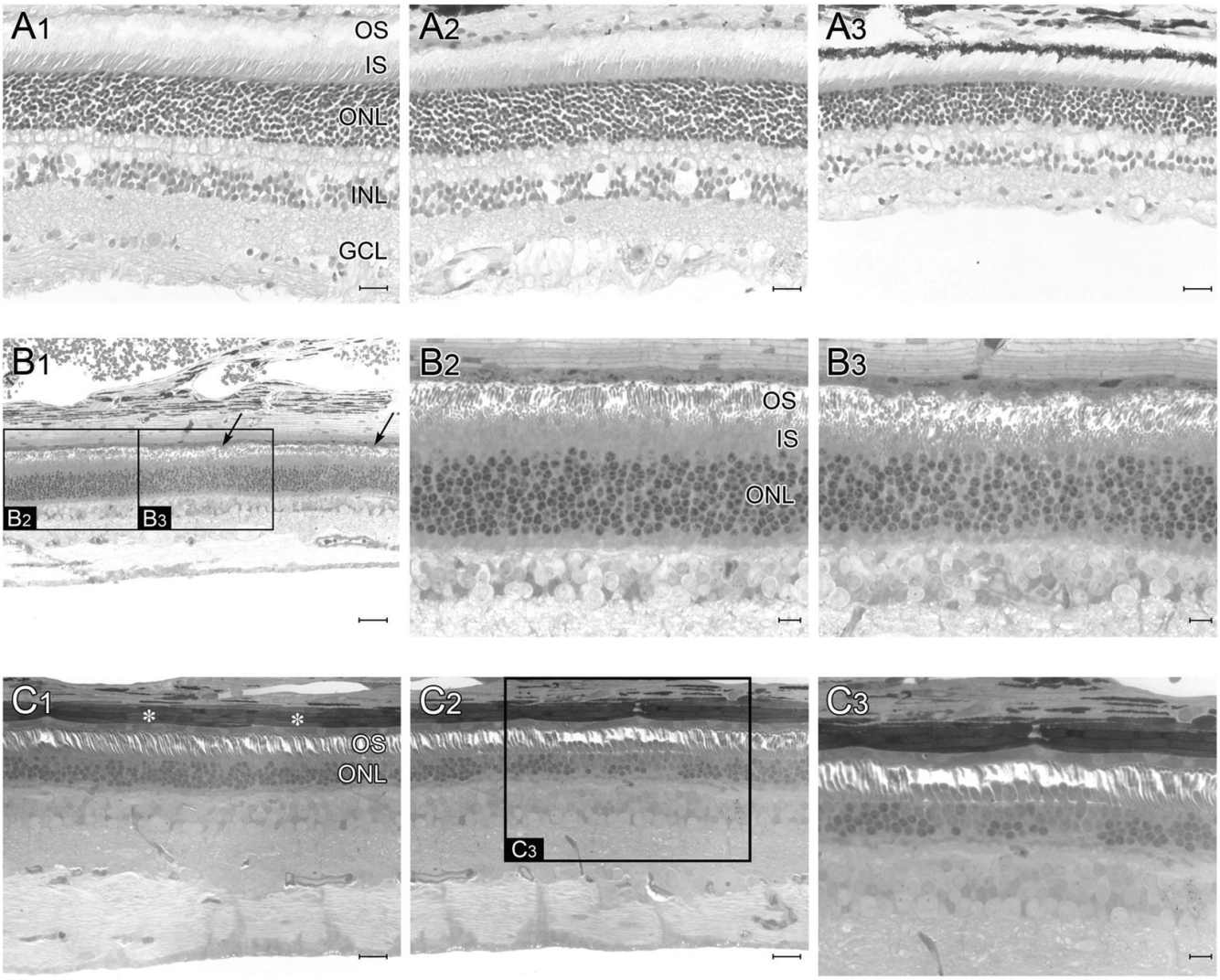

Figure 2.

Retinal morphology in carriers of *XLPRA1*. (**$A_{1–3}$**) H&E stained retinal cryosections along the superior meridian of a 24 week-old carrier of *XLPRA1*. No morphologic abnormalities are detected at this age in the central (**A_1**), mid-peripheral (**A_2**), and peripheral (**A_3**) regions. (**$B_{1–3}$**) Epoxy resin retinal section of a 1.4 year-old carrier of *XLPRA1*. (**B_1**) Focal patches (arrows) of retinal degeneration are found throughout the retina. In these areas, there is a loss of OS, shortening and broadening of IS and a decrease in ONL cell density (**B_3**) and contrast with surrounding areas (**B_2**) that have a better preserved morphology. (**$C_{1–3}$**) Epoxy resin retinal section of a 7.9 year-old carrier of *XLPRA1*. (C_1) A generalized thinning of the ONL is seen throughout the retina, yet remaining photoreceptors maintain their normal IS and OS (asterisks). (**C_2**) Focal area of severe ONL thinning. (**C_3**) Higher magnification of C_2 insert. In this foci note the increased number of cone IS and nuclei, and the reduced density of rods. Scale bars: ($B_{2–3}$) 10 μm; ($A_{1–3}$, $C1_{–2}$) 20 μm; (B_1, C_3) 40 μm.

Abbreviations: OS = outer segments; IS = inner segments; ONL = outer nuclear layer; INL = inner nuclear layer; GCL = ganglion cell layer.

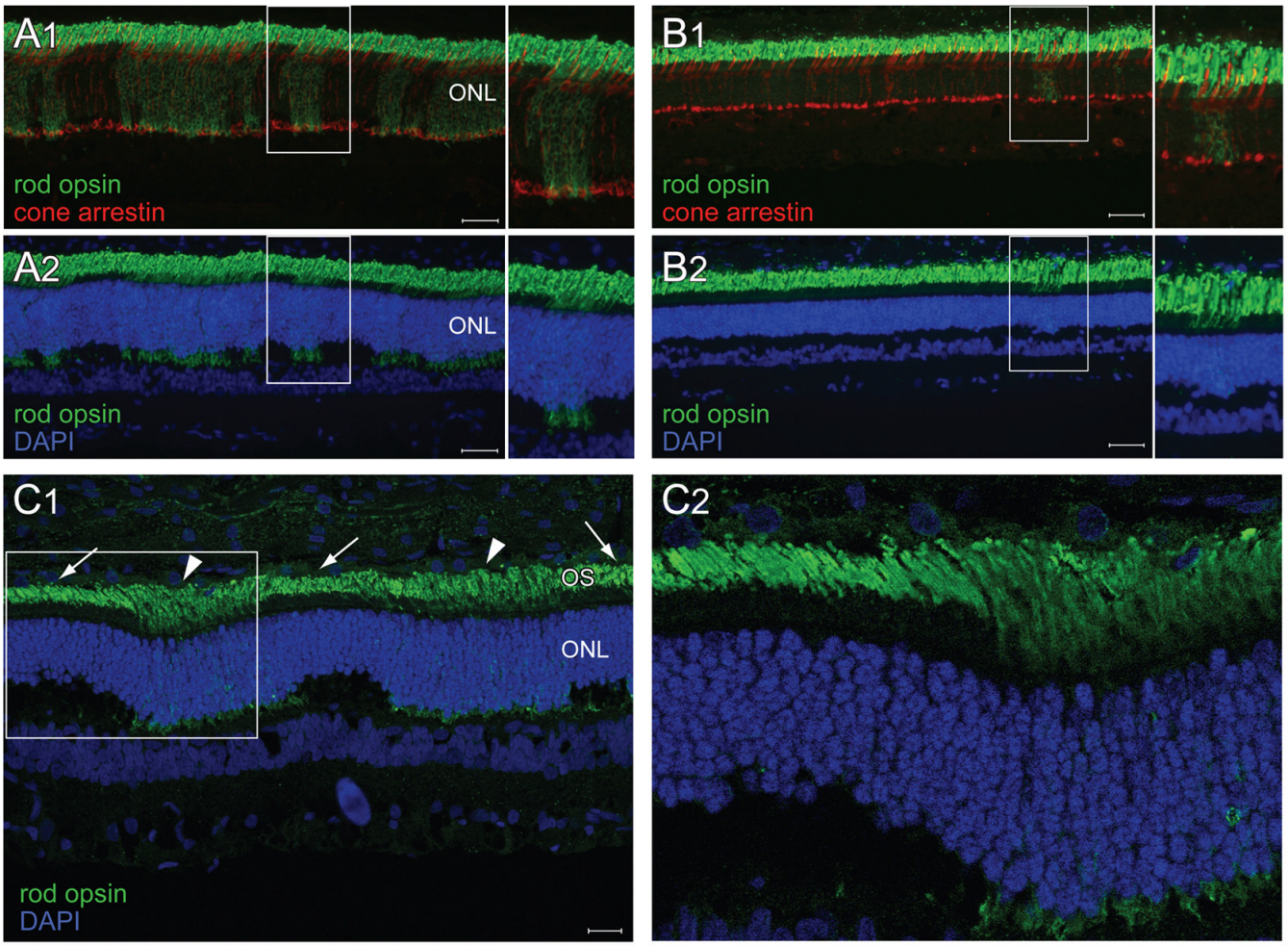

Figure 3.

Disease and remodeling of the rod photoreceptor mosaic in carriers of *XLPRA2*. (**$A_{1–2}$**) Double fluorescence immunohistochemistry in a 4.9 week-old *XLPRA2* carrier shows numerous patches of rod opsin (green) mislocalization to the inner segments and ONL but no abnormalities in cone arrestin labeling (red) (**A_1**). Co-labeling with DAPI nuclear stain (blue) shows that patches of rod opsin mislocalization and rod neurite sprouting (see arrow in insert) occur in areas of ONL thickening (**A_2**). Double fluorescence immunohistochemistry in a 39 week-old *XLPRA2* carrier shows a single patch of rod opsin (green) mislocalization to the inner segments and persistent normal expression of cone arrestin (**B_1**). DAPI nuclear stain shows that the overall ONL thickness is reduced (**B_2**). The inner margin of the ONL is less wavy than at earlier ages. However persistent focal regions of ONL thickening are seen at the sites of rod opsin mislocalization (**B_2**). Rod opsin and DAPI labeling in a 5.9 week-old XLPRA2 carrier imaged by confocal microscopy (maximal projection reconstituted image) (**C_1**). Note the disorganized OS (arrowheads) in the patches of opsin mislocalization and ONL thickening, which contrast with the aligned rod OS (arrows) in adjacent areas of non-diseased retina. Insert seen in C1 is shown as a single plane image at higher magnification in (**C_2**). Scale bars $A_{1–2}$, $B_{1–2}$: 40 μm; C_1: 20 μm. Abbreviations: ONL = outer nuclear layer; OS = outer segments.

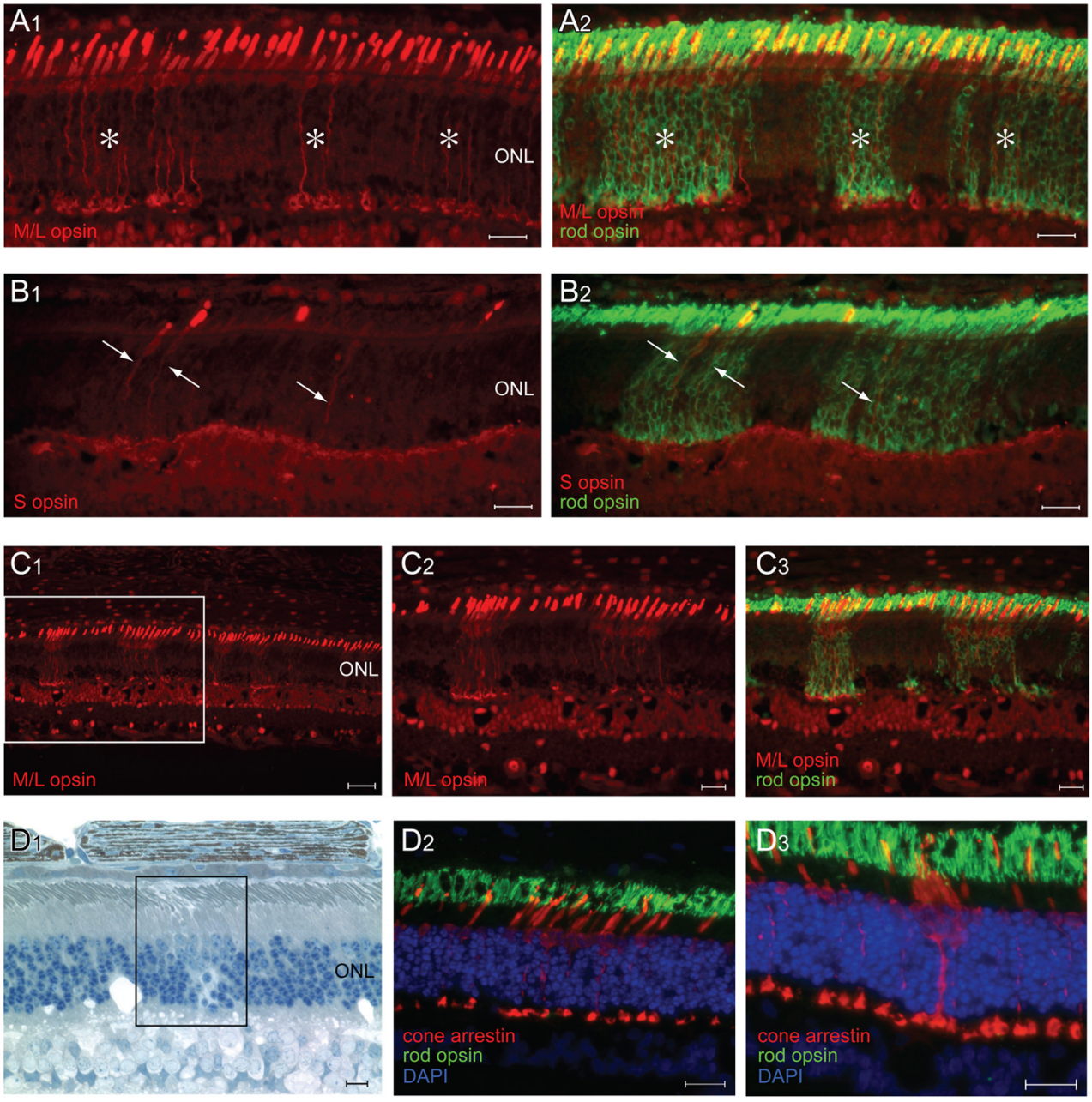

Figure 4.

Disease and remodeling of the cone photoreceptor mosaic in carriers of *XLPRA2*. Double fluorescence immunohistochemistry in a 4.9 week-old *XLPRA2* carrier shows M/L opsin mislocalization to the inner segments, ONL and cone pedicle (**A_1**) in the same patches where rod opsin is mislocalized (see asterisks) (**A_2**). (Note 1: the labeling of the inner retina with the M/L opsin antibody is not specific. Note 2: the yellow labeling seen in the cone outer segments is the result of a post-acquisition increase in the green signal of the overlay image to improve visualization of the rod opsin mislocalization, and does not represent co-localization). In a 5.9 week-old *XLPRA2* carrier, faint S opsin mislocalization to the inner segments, and ONL is seen in some cones (arrows) (**B_1**). These cones are located within patches of rod opsin mislocalization (**B_2**). Immunolabeling in a 5.9 week-old *XLPRA2* carrier show an increased

density in M/L cones in the patches of rod and M/L opsin mislocalization (**$C_{1–3}$**). (**D_1**) Plastic embedded retinal section of a 26.1 week-old *XLPRA2* carrier showing focal accumulation of large euchromatic nuclei resembling that of cones in an area of rod loss. (**$D_{2–3}$**) Double fluorescence IHC in a 39 week-old *XLPRA2* carrier showing increased density of cones that can either be distributed in a monolayer (**D_2**) or clumped together (**D_3**). Note that there is no rod opsin mislocalization in the patches of increased cone density. Scale bars : (D_1) 10 μm; ($A_{1–2}$, $B_{1–2}$, $C_{2–3}$, $D_{2–3}$) 20 μm; (C_1) 40 μm. Abbreviations: ONL = outer nuclear layer.

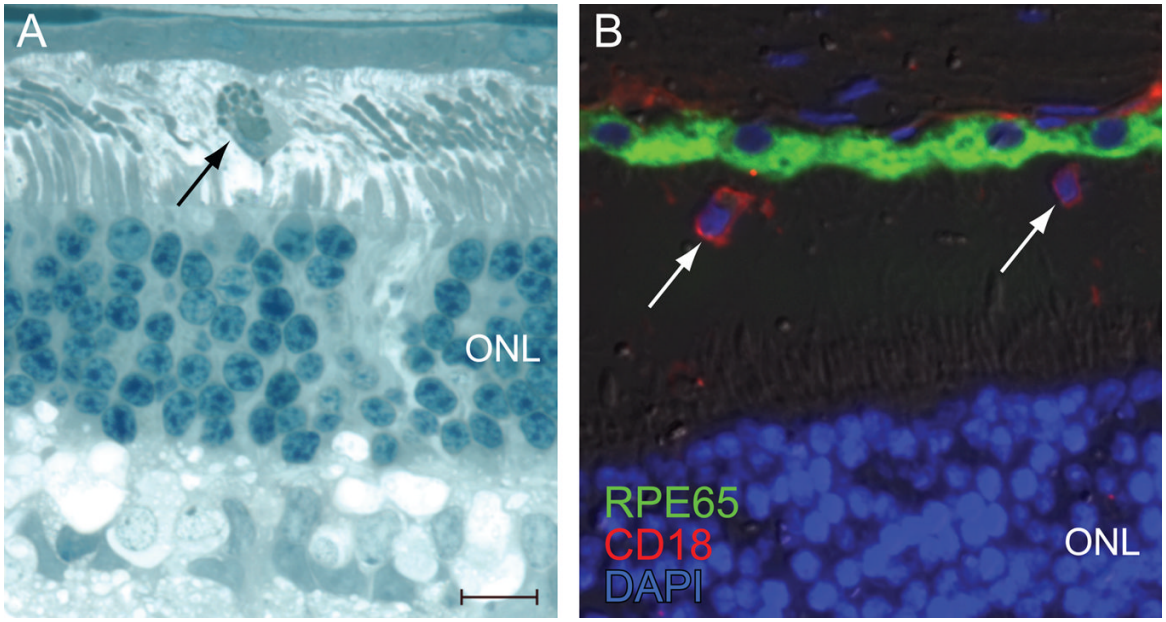

Figure 5.

Focal invasion of the subretinal layer by phagocytic cells in carriers of *XLPRA2* (**A**) Plastic embedded retinal section of a 26.1 week-old *XLPRA2* dog showing a phagocytic cell in the subretinal space overlying a patch of degeneration. Note the multiple cytoplasmic inclusions suggestive of phagocytized rod disc material. (**B**) Double fluorescent IHC in this same animal labels shows that these cells are labeled with CD18 but not with RPE65 antibodies. This confirms their macrophage origin. Scale bar: 10 μm. Abbreviations: ONL = outer nuclear layer.

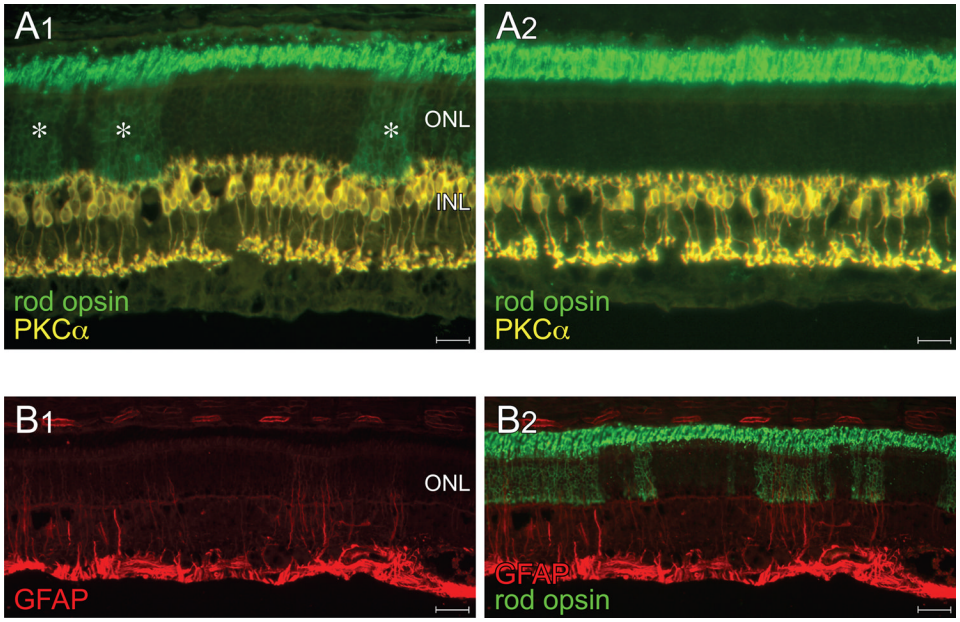

Figure 6.

Disease and remodeling of the inner retinal mosaic in carriers of *XLPRA2* at 7.9 and 39 weeks of age. Double fluorescence IHC in a 7.9 week-old *XLPRA2* carrier shows focal dendritic retraction of rod bipolar cells (yellow) beneath the patches of rod opsin mislocalization (asterisks) (**A_1**). Absence of rod bipolar dendritic retraction is noted in the 39 week-old *XLPRA2* carrier (**A_2**). (**$B_{1–2}$**) GFAP immunohistochemistry in a 7.9 week-old *XLPRA2* carrier shows patchy labeling of the radial extensions of reactive Müller cells (**B_1**). Double IHC confirms that these GFAP labeled radial extensions occur in Müller cells located beneath the larger patches of rod opsin mislocalization (**B_2**). Scale bars: ($A_{1–2}$) 20 μm; ($B_{1–2}$) 40 μm. Abbreviations: ONL = outer nuclear layer; INL = inner nuclear layer.

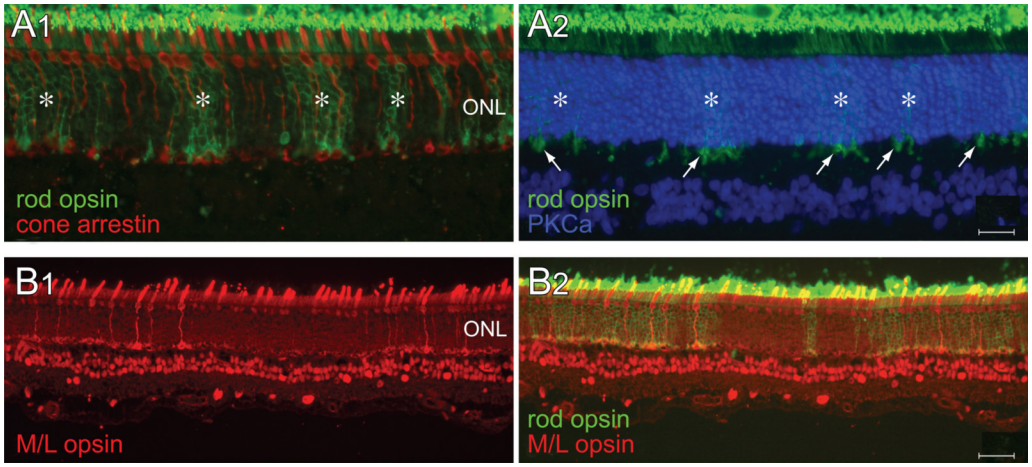

Figure 7.

Photoreceptor mosaic in the *XLPRA1* carrier. (**$A_{1–2}$**) Double fluorescence immunohistochemistry in a 24 week-old *XLPRA1* carrier shows numerous patches of rod opsin (green) mislocalization to the inner segments and ONL (asterisks), but no abnormalities in cone arrestin labeling (red) (**A_1**). Co-labeling with DAPI nuclear stain (blue) shows patches of rod opsin mislocalization and rod neurite sprouting (see arrows) (**A_2**).(**$B_{1–2}$**) Double fluorescence immunohistochemistry in a 24 week-old *XLPRA1* carrier shows M/L opsin mislocalization to the inner segments, ONL and cone pedicle (**B_1**) in the same patches where rod opsin is mislocalized (**B_2**). Note that M/L opsin labeling of the inner nuclear layer and ganglion cell layer is non-specific. Scale bars: ($A_{1–2}$) 20 μm; ($B_{1–2}$) 40 μm. Abbreviations: ONL = outer nuclear layer.

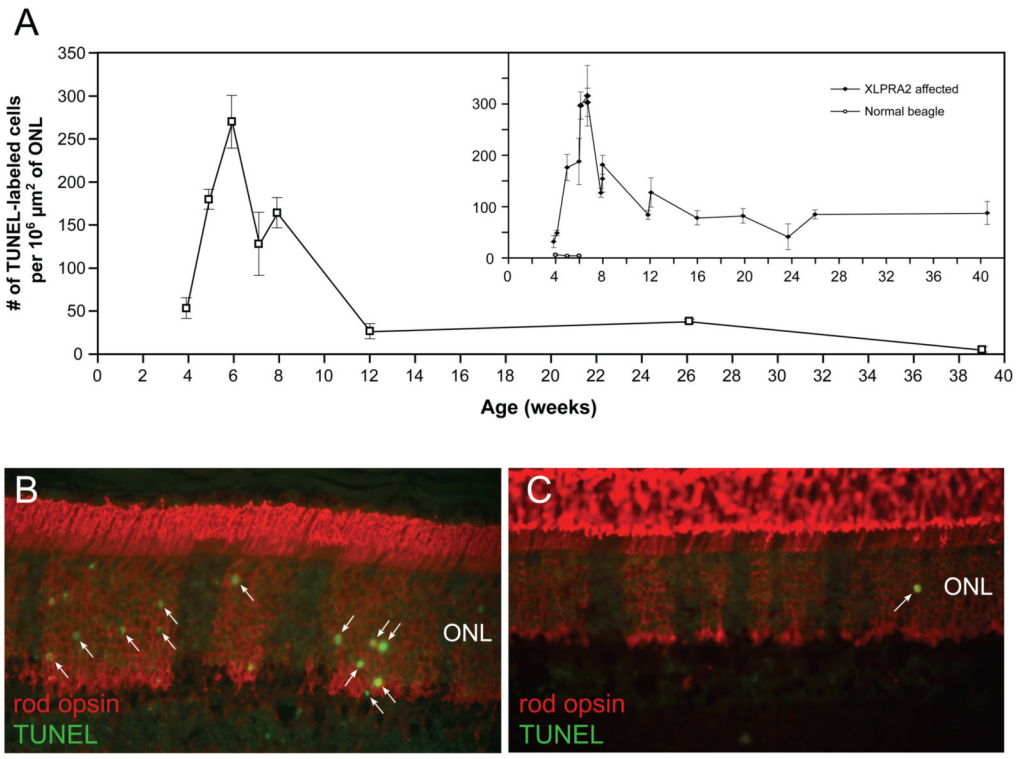

Figure 8.

Photoreceptor cell death in carriers of XLPRA. (**A**) Kinetics of photoreceptor cell death in the superior meridian of *XLPRA2* carriers. The insert shows previously published (Beltran et al, *IOVS*, 2006) kinetics of cell death in affected XLPRA2 dogs. (**B**) TUNEL labeling of rod nuclei (arrows) in a 4.9 week-old *XLPRA2* carrier is seen exclusively in the patches of rod opsin mislocalization. (**C**) Single TUNEL-labeled rod in a 24 week-old *XLPRA1* carrier is located in a patch of rod opsin mislocalization. Abbreviations: ONL = outer nuclear layer.

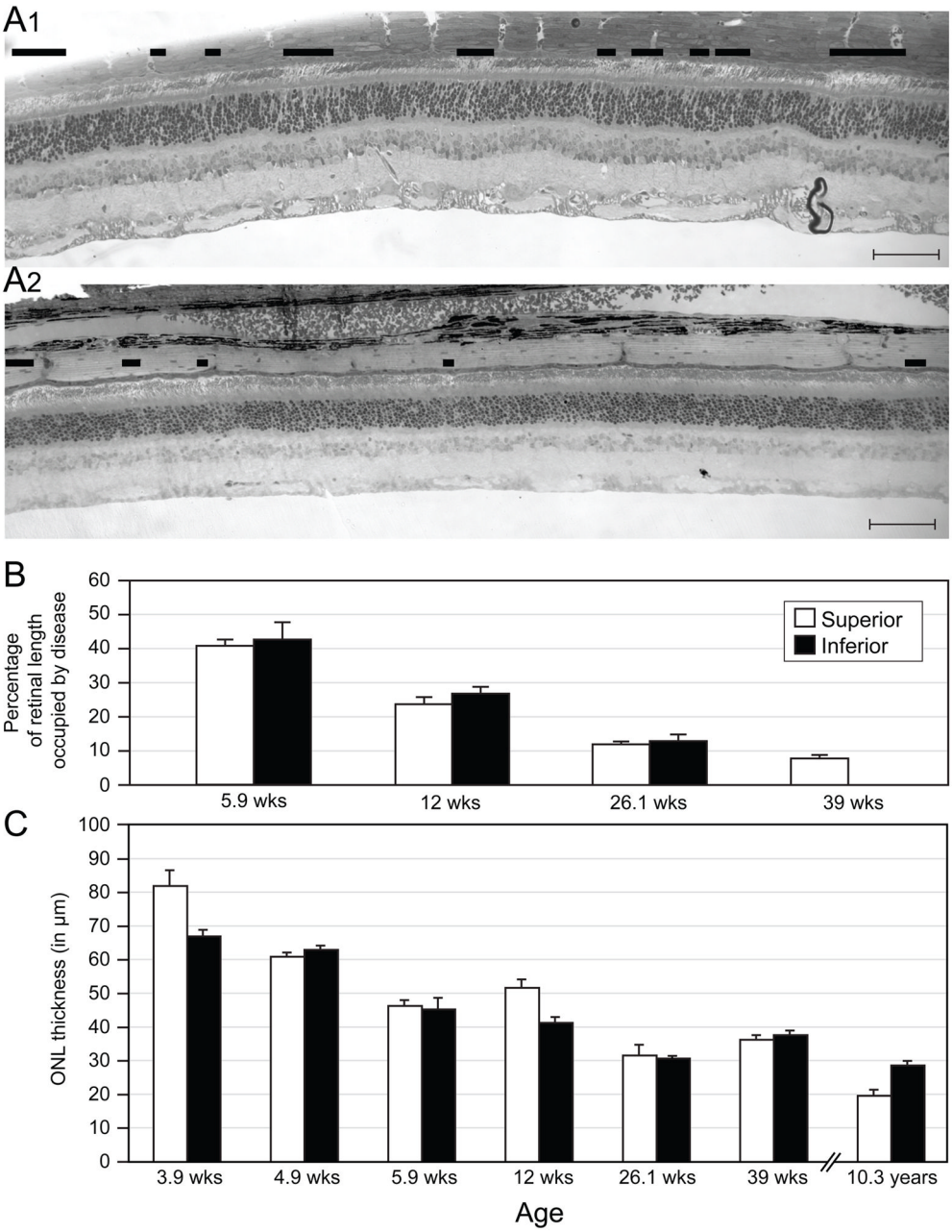

Figure 9.

Remodeling of the retinal mosaic in carriers of *XLPRA2*. (**A_1**) Numerous foci of retinal disease (horizontal black bars) occupy a significant proportion of the retinal length as seen here in the mid-peripheral region of the superior retina of a 5.9 week-old carrier of *XLPRA2*. (**A_2**) Infrequent and small foci of retinal disease are found at later ages as illustrated here in the mid-peripheral region of the superior retina of a 39 week-old carrier of *XLPRA2*. (**B**) Percentage (mean ± SD) of the total retinal length along the superior and inferior meridians that is occupied by foci of retinal disease in carriers of *XLPRA2* of different ages. (**C**) Mean (±SD) ONL thickness in the mid-peripheral region of the superior and inferior meridians in XLPRA2 carriers of different ages. Note that ONL thickness was measured in areas between patches of disease. Scale bars: 10 µm.

Table 1

List of dogs used for the morphologic, TUNEL, and immunohistochemistry studies.

ID	Age	Morphology	TUNEL	IHC
XLPRA2 carrier				
Z277	3.9 weeks	EPON	+	+
Z278	4.9 weeks	EPON	+	+
Z279	5.9 weeks	EPON	+	+
Z274	7.1 weeks	OCT	+	+
Z280	7.9 weeks	OCT	+	+
Z225	12 weeks	EPON	+	+
Z184	26.1 weeks	EPON	+	+
Z199	39 weeks	EPON	+	+
Z87	8.8 Years	OCT		
Z24	10.3 Years	EPON		
XLPRA1 carrier				
H408	20 weeks	OCT	+	+
H414	24 weeks	OCT	+	+
H237 (40)*	1.4 Year	EPON		
H6 (3)*	3.5 Years	EPON		
H74 (18)*	3.8 Years	EPON		
H43 (8)*	4.9 Years	EPON		
H44 (7)*	5.7 Years	EPON		
H25 (4)*	6 Years	EPON		
H4 (2)*	7.8 Years	EPON		

Morphologic assessment was done either on epoxy resin (EPON) embedded sections or on OCT (OCT) embedded cryosections.

IHC: immunohistochemistry; +: done;

*Number in parenthesis corresponds to identification used in Zeiss et al. *IOVS* (1999).

Table 2

List of primary antibodies used in this study.

Antigen	Host	Source, catalog # or name	Working concentration	Normal retinal localization
RPE65	rabbit	T.M. Redmond	1:10,000	Retinal pigment epithelium
Human cone arrestin	rabbit	C. Craft, LUMIF	1:10,000	Cone photoreceptors
M/L cone opsin	Rabbit polyclonal	Chemicon, AB5405	1:500	OS of M/L cones
S cone opsin	Rabbit polyclonal	Chemicon, AB5407	1:500	OS of S cones
Rod opsin	Mouse monoclonal	Chemicon, MAB5316	1:1,000	OS of rods
Synaptophysin	Rabbit polyclonal	DakoCytomation, A0010	1:100	Neuron synapses, OPL, IPL
Protein Kinase C (PKCα)	Mouse monoclonal IgG2b	BD Biosciences, 610107	1:100	Rod bipolar cells
Goα	Mouse monoclonal IgG1	Chemicon, MAB3073	1:5,000	ON (rod and cone) bipolar cells
γ-amino butyric acid (GABA)	Rabbit polyclonal	Chemicon, AB5016	1:50	GABAergic amacrine cells
Glial Fibrillary acidic protein (GFAP)	Rabbit polyclonal	DakoCytomation, Z0334	1:1,000	Astrocytes, Müller cells (reactive)
Glutamine synthetase	Mouse monoclonal	Chemicon, MAB302	1:20,000	Müller cells
CD-18	Mouse monoclonal IgG1	Leukocyte antigen lab, UC Davis	1:10	None unless disease

Table 3

Thickness of the ONL (mean number of rows of ONL nuclei) in the central (S1), mid-peripheral (S2) and peripheral (S3) retina of *XLPRA2* carriers.

ID	Age	S1	S2	S3	Retinal length
XLPRA2 carrier					
Z277	3.9 weeks				
Superior		ND	ND	ND	ND
Inferior		11–12	11	10	7,500
Z278	4.9 weeks				
Superior		11–12	10–11	9–10	12,600
Inferior		12	10	9	8,750
Z279	5.9 weeks				
Superior		10	8	7	11,700
Inferior		8	8	7	9,200
Z225	12 weeks				
Superior		11	10	ND	14,000
Inferior		9	8	7	10,700
Z184	26.1 weeks				
Superior		6	6	5	16,400
Inferior		6–7	6–7	5–6	11,000
Z199	39 weeks				
Superior		7	7	7	15,000
Inferior		8	7	6	12,000
Z87	8.8 Years				
Superior		5–6	4–5	0	15,600
Inferior		3	3	0	11,400
Z24	10.3 Years				
Superior		6	0	0	13,700
Inferior		7	5	5	12,000

ND: not determined.

Table 4

Central and peripheral ONL thickness (mean number of rows of ONL nuclei/site) along the superior meridian of *XLPRA1* carrier retinas.

ID	Age	Central	peripheral
XLPRA1 carrier			
H408	20 weeks	9	7
H414	24 weeks	9	6–7
H237	1.4 years	9	3–4
H6	3.5 Years	9	3
H74	3.8 years	5	0
H43	4.9 years	6–7	3–4
H44	5.7 years	5	2–3
H25	6 Years	5	1–2
H4	7.8 Years	5	4–5

Table 5

Summary of morphologic changes in carriers and affected dogs of two models of X-linked retinitis pigmentosa.

	XLPRA1	XLPRA2
Mutation in *RPGR*ORF15 and putative effect	Del (1028–1032) causes a premature stop Loss of function	Del (1084–1085) causes a frameshift Toxic gain of function
Carriers (current study)		
Time course of patchy disease/degeneration	Observed between 20 weeks and 7.8 years	3.9 – 39 weeks
Peak of cell death	ND	5.9 weeks
ONL thickness in patches of disease		
Early	Unchanged	Increased
Late	Decreased	Uniform decrease (no patchy disease)
Opsin (rod, M/L, S) mislocalization	Yes	Yes
Clumping of cones in patches of disease	Yes	Yes
Inner retina remodeling below patches of disease	ND	Yes (observed at 7.9 weeks)
Tangential displacement of non-mutant rods into patches of disease.	Limited	Yes
Phagocytic cells in subretinal space	ND	Yes
(mid) peripheral retinal atrophy at later stages	Yes	Yes
Affected22¯24, 43		
Onset of disease	11 months	3.9 weeks
Peak of cell death	ND	6–7 weeks
Progression of disease	Slow	Rapid
Opsin (rod, M/L, S) mislocalization	ND	Yes
Inner retina remodeling	ND	Yes (observed at 11.9 weeks)
Phagocytic cells in subretinal space	Yes	Yes

ND: not determined